# Loss of the mucosal barrier alters the progenitor cell niche via Janus kinase/signal transducer and activator of transcription (JAK/STAT) signaling

Received for publication, August 1, 2017, and in revised form, October 23, 2017 Published, Papers in Press, November 10, 2017, DOI 10.1074/jbc.M117.809848

**Liping Zhang**[‡], **Bradley Turner**[§1], **Katharina Ribbeck**[§1], **and Kelly G. Ten Hagen**[‡2]

*From the* [‡]*Developmental Glycobiology Section, NIDCR, National Institutes of Health, Bethesda, Maryland 20892-4370 and the* [§]*Department of Biological Engineering, Massachusetts Institute of Technology, Cambridge, Massachusetts 02139*

Edited by Gerald W. Hart

**The mucous barrier of our digestive tract is the first line of defense against pathogens and damage. Disruptions in this barrier are associated with diseases such as Crohn's disease, colitis, and colon cancer, but mechanistic insights into these processes and diseases are limited. We have previously shown that loss of a conserved *O*-glycosyltransferase (PGANT4) in *Drosophila* results in aberrant secretion of components of the peritrophic/mucous membrane in the larval digestive tract. Here, we show that loss of PGANT4 disrupts the mucosal barrier, resulting in epithelial expression of the IL-6–like cytokine Upd3, leading to activation of JAK/STAT signaling, differentiation of cells that form the progenitor cell niche, and abnormal proliferation of progenitor cells. This niche disruption could be recapitulated by overexpressing *upd3* and rescued by deleting *upd3*, highlighting a crucial role for this cytokine. Moreover, niche integrity and cell proliferation in *pgant4*-deficient animals could be rescued by overexpression of the conserved cargo receptor Tango1 and partially rescued by supplementation with exogenous mucins or treatment with antibiotics. Our findings help elucidate the paracrine signaling events activated by a compromised mucosal barrier and provide a novel *in vivo* screening platform for mucin mimetics and other strategies to treat diseases of the oral mucosa and digestive tract.**

The mucous barrier that lines our respiratory and digestive tracts is the first line of defense against pathogens and provides hydration and lubrication (1–4). This unique membrane separates the delicate epithelia from factors present in the external environment. In mammals, the mucous lining of the intestine allows nutrient penetration while conferring protection from both bacteria and the mechanical damage associated with digestion of solid food (reviewed in Refs. 2 and 5). The principal components of mucous membranes are mucins, a diverse family of proteins that are expressed in tissue-specific fashions (2, 5–8). Whereas secreted mucins vary greatly in sequence and size, they all share highly *O*-glycosylated serine- and threonine-rich regions that confer unique structural and rheological properties, allowing the formation of hydrated gels. Deletion of specific components of the mucous membranes present in the lung (Muc5b (9)) or the intestinal tract (Muc2 (10)) resulted in defects in mucociliary clearance or an increased incidence colorectal cancer, respectively. Changes in mucus production or the glycosylation status of mucins have also been associated with oral pathology in Sjogren's syndrome (11, 12), the development of colitis and intestinal tumors in mice (10, 13–15), and the progression of ulcerative colitis and colon cancer in humans (16, 17). However, the detailed mechanisms by which loss/alteration of this protective layer results in epithelial pathology remain unknown.

Many components and factors that confer the unique properties of this protective lining, including the mucins and the enzymes that mediate their dense glycosylation, are conserved across species (18–21). Indeed, *Drosophila melanogaster* contains a similar protective lining known as the peritrophic membrane, consisting of a chitin scaffold that is bound by highly *O*-glycosylated mucins (8, 22). During larval development, where animals ingest solid food and undergo massive growth in preparation for metamorphosis, specialized secretory cells (PR cells) of the anterior midgut produce this membrane, which is thought to protect epithelial cells of the digestive tract from mechanical and microbial damage (22, 23). Previous work in *Drosophila* has shown that loss of one component of the peritrophic membrane resulted in a thinner and more permeable membrane, where adult flies were viable yet more susceptible to oral infections (24). However, the exact role of the entirety of this lining in the integrity and protection of cells of the digestive tract remains unknown.

Extensive research elucidating the development and function of the many cell types that comprise the *Drosophila* digestive tract has provided insights into mammalian digestive system formation and function (23, 25–27). The *Drosophila* larval midgut is composed of specialized epithelial cells (enterocytes (ECs)[3] and enteroendocrine cells) for digestion and nutrient

This work was supported by the Intramural Research Program of NIDCR, National Institutes of Health, Grant Z01-DE-000713 (to K. G. T. H.). The authors declare that they have no conflicts of interest with the contents of this article. The content is solely the responsibility of the authors and does not necessarily represent the official views of the National Institutes of Health.

This article contains Figs. S1–S5.

[1] These authors were supported through the Materials Research Science and Engineering Center Program of the National Science Foundation (NSF) (Grant DMR-0819762), NSF CAREER Award PHY-1454673, and National Institutes of Health Grant RO1-EB017755 (to K. R.).

[2] To whom correspondence should be addressed: Bldg. 30, Rm. 426, 30 Convent Dr., MSC 4370, Bethesda, MD 20892-4370. Tel.: 301-451-6318; Fax: 301-402-0897; E-mail: Kelly.Tenhagen@nih.gov.

[3] The abbreviations used are: EC, enterocyte; PC, peripheral cell; AMP, adult midgut progenitor cell; PH3, phosphohistone H3; CMC, carboxymethylcellulose; VDRC, Vienna *Drosophila* RNAi Center; DIG, digoxigenin.

absorption, as well as progenitor cells that will eventually form the adult midgut epithelium (26, 28, 29). These adult midgut progenitor cells (AMPs) reside in a protected niche, formed by peripheral cells (PCs) that wrap and shield them from external signaling (28). PCs are characterized by a unique crescent shape, with long processes that surround AMPs, restricting proliferation and differentiation until metamorphosis (25). The larval digestive tract therefore represents an ideal system to interrogate the role of the mucous layer in protection of both the epithelium and the progenitor cell niche at a stage when the mechanical and microbial stresses associated with the ingestion of solid food are abundant.

Previous work from our laboratory has shown that loss of a conserved UDP-GalNAc:polypeptide *N*-acetylgalactosaminyltransferase responsible for initiating *O*-linked glycosylation (PGANT4) resulted in aberrant secretion of components of the peritrophic membrane in the larval digestive tract (30). Here, we show that *pgant4* mutants are devoid of a peritrophic membrane, resulting in epithelial cell damage and expression of the IL-6–like inflammatory cytokine, unpaired 3 (Upd3). Upd3 expression resulted in increased JAK/STAT signaling in the progenitor cell niche, causing niche cell differentiation and aberrant progenitor cell proliferation. These effects were dependent on Upd3 and could be rescued by deleting *upd3* or partially rescued by feeding animals antibiotics or exogenous mammalian intestinal mucins. Moreover, overexpression of the conserved extracellular matrix cargo receptor, Tango1 (transport and Golgi organization 1), in secretory cells of the digestive tract resulted in restoration of the peritrophic membrane and rescue of niche integrity. Our results elucidate new mechanistic details regarding how a compromised mucous lining can influence epithelial integrity and the progenitor cell niche and provide an *in vivo* screening platform for compounds and strategies that could restore mucosal barrier function.

## Results

To address the role of the mucosal barrier in normal digestive system health, we examined third instar *Drosophila* larvae deficient for *pgant4*, which were previously shown to have defects in the formation of secretory vesicles in the PR cells that are responsible for the synthesis and secretion of the peritrophic membrane (30). Loss of *pgant4*, via conventional mutations ($pgant4^{f02186}/Df2L$) or *in vivo* RNAi specifically in PR cells ($c135>pgant4^{RNAi}$) resulted in complete loss of the peritrophic membrane throughout the larval digestive tract (Fig. 1*A* and Fig. S1). The lectin *Helix pomatia*, which detects GalNAc linked to serine or threonine, revealed specific loss of *O*-glycosylated proteins/mucins along the surface of the epithelium (Fig. 1*A*). Staining with the chitin-binding protein (Chitin) revealed loss of all chitin normally present as part of the peritrophic membrane along the digestive tract (Fig. S1*A*). Additionally, larvae fed fluorescently labeled dextran showed that in WT, food was encased in the protective peritrophic membrane, but no food encasement was seen in *pgant4* mutants (Fig. S1*B*). Loss of the peritrophic membrane resulted in epithelial irregularities within the midgut (as detected by actin, which outlines cells), where cells no longer form a single cell layer but rather a multicell layer in places, with some cells detaching (Fig. 1, *A* and *B*). Additionally, loss of the peritrophic membrane resulted in the induction of epithelial apoptosis (as detected by the caspase marker, Dcp-1) (Fig. 1*B*) and the up-regulation of certain genes encoding antimicrobial proteins (Fig. 1*E*).

In addition to epithelial apoptosis, increased cell proliferation within the midgut was detected by EdU and phosphohistone H3 (PH3) staining upon loss of the peritrophic membrane (Fig. 1*C* and Fig. S2). Co-staining with PH3 and markers for the various cell types of the digestive tract, including PCs (detected by the marker Su(H)-lacZ) and AMPs (detected by the marker Delta), revealed that the proliferating cells were the AMPs (Fig. 1*D* and Fig. S3). During normal larval development, AMPs undergo limited proliferation and remain in an undifferentiated state within the unique progenitor cell niche formed by the PCs (Fig. 2*A*). Interestingly, niche morphology was altered in *pgant4* mutants (Fig. 2*B*). The normally crescent-shaped PCs were found to be in various stages of flattening/rounding and unwrapping AMPs. Once unwrapped, AMPs, which normally exist as tight groups of cells that stain brightly for the marker Armadillo (Arm) around their periphery in WT, were no longer present in tight groupings in *pgant4* mutants (Fig. 2*C*). In addition to changes in PC morphology, we also observed changes in PC fate in *pgant4* mutants. PCs are normally positive for the marker Su(H), whereas differentiated ECs are positive for the marker Pdm-1 (Fig. 2*D*). However, upon loss of the peritrophic membrane, many Su(H)-positive PCs were also positive for Pdm-1 (Fig. 2, *D* and *E*), suggesting that PCs are undergoing differentiation to EC-like cells. Taken together, these data indicate that loss of the peritrophic membrane affects PC differentiation and morphology, suggesting important roles for this protective membrane in maintenance of the progenitor cell niche.

We next performed qPCR analysis to determine which signaling pathways might be responsible for the changes in PC fate. Interestingly, a specific and dramatic increase in the expression of the gene encoding the IL-6–like inflammatory cytokine (and ligand for JAK/STAT signaling) unpaired 3 (*upd3*) and its downstream target *socs36E* were observed (Fig. 3*A*). Other signaling pathways known to be involved in response to damage within the digestive system of *Drosophila* did not show consistent and significant changes (Fig. S4). These results suggest that loss of the protective lining is activating JAK/STAT signaling through the production of Upd3 (but not Upd or Upd2). To determine the source of Upd3, we performed RNA *in situ* hybridizations to *upd3* in WT and *pgant4* mutant midguts. As shown in Fig. 3*B*, *upd3* expression is not normally detected in WT but is up-regulated in the large ECs (characterized by large nuclei) of the midgut upon loss of *pgant4* and the peritrophic membrane.

Upd3 production from ECs upon loss of the peritrophic membrane could activate JAK/STAT signaling in an autocrine or paracrine manner. To determine in which cells Upd3 is activating JAK/STAT signaling, we next performed RNAi to *pgant4* in a reporter line that contains 10 STAT-binding sites driving GFP expression (Stat92E-GFP). Using this line, cells in which JAK/STAT signaling is activated will fluoresce green. Interestingly, PCs of the progenitor cell niche showed a dra-

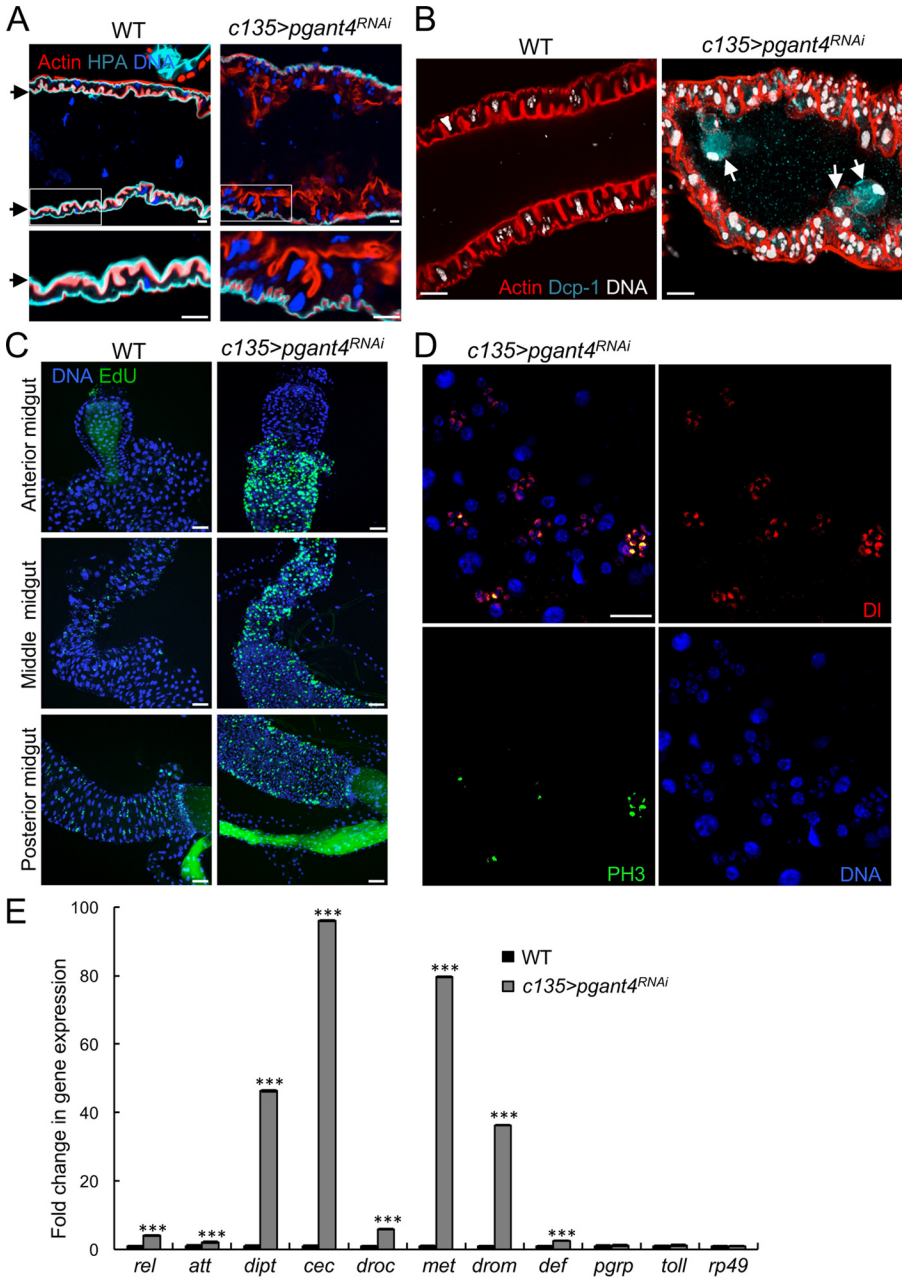


**Figure 1. Loss of the peritrophic membrane causes epithelial cell apoptosis and progenitor cell proliferation.** *A*, the peritrophic membrane (as detected by the lectin *H. pomatia*; *cyan*) that coats the epithelial cells of the WT (*c135>VDRC60000*) midgut is lost upon knockdown of *pgant4* (*c135>pgant4$^{RNAi}$*). The epithelial cell layer of the digestive tract (outlined with actin; *red*) is disorganized upon loss of the peritrophic membrane. *Magnified views* of *insets* are shown *below* each image. Nuclear staining is shown in *blue*. *Scale bars*, 20 μM. *B*, loss of the peritrophic membrane (*c135>pgant4$^{RNAi}$*) results in increased epithelial apoptosis, as detected by the apoptosis marker, Dcp-1 (*cyan*). The epithelial cell layer is outlined by actin staining (*red*), and nuclei are *white*. *White arrows* indicate cells that are detached and/or undergoing apoptosis. *Scale bars*, 20 μM. *C*, loss of the peritrophic membrane (*c135>pgant4$^{RNAi}$*) results in increased cell proliferation throughout the anterior, middle, and posterior midgut regions relative to WT, as detected by EdU (*green*). *Scale bars*, 50 μM. *D*, phosphohistone H3-positive (*PH3*, *green*) proliferating cells are the AMPs that are detected by the Delta marker (*Dl*, *red*). ECs are those with the large nuclei (*DNA*, *blue*). *Scale bar*, 10 μM. *E*, loss of the peritrophic membrane results in up-regulation of antimicrobial gene expression. qPCR analysis of antimicrobial gene expression was performed on cDNA synthesized from RNA extracted from WT and *c135>pgant4$^{RNAi}$* third instar midguts. Values were normalized to *rp49* and are plotted as -fold change in gene expression. *Error bars*, S.D. ***, $p < 0.001$.

matic increase in JAK/STAT signaling in the absence of the peritrophic membrane (*c135>pgant4$^{RNAi}$*) relative to WT (Fig. 3*C*). In WT midguts, islands of cells consist of JAK/STAT-negative AMP clusters (small nuclei) surrounded by JAK/STAT-positive PCs (medium-sized, green nuclei) (Fig. 3*C*). Upon loss of the peritrophic membrane, large clusters of cells consisting of both medium-sized nuclei (PCs) and small nuclei (AMPs) fluoresced brightly for JAK/STAT signaling (Fig. 3*C*). ECs with large nuclei remained negative for JAK/STAT signaling in both WT and *c135>pgant4$^{RNAi}$* midguts (Fig. 3*C*), indicating that Upd3 is not acting in a cell-autonomous manner. Notably, some cells with small nuclei that appeared to remain surrounded by PC processes remained JAK/STAT negative, suggesting that residual PC wrapping might protect some AMPs from external Upd3 signals (Fig. 3*C*, *red arrow*). These data suggest that a dramatic up-regulation in JAK/STAT signaling

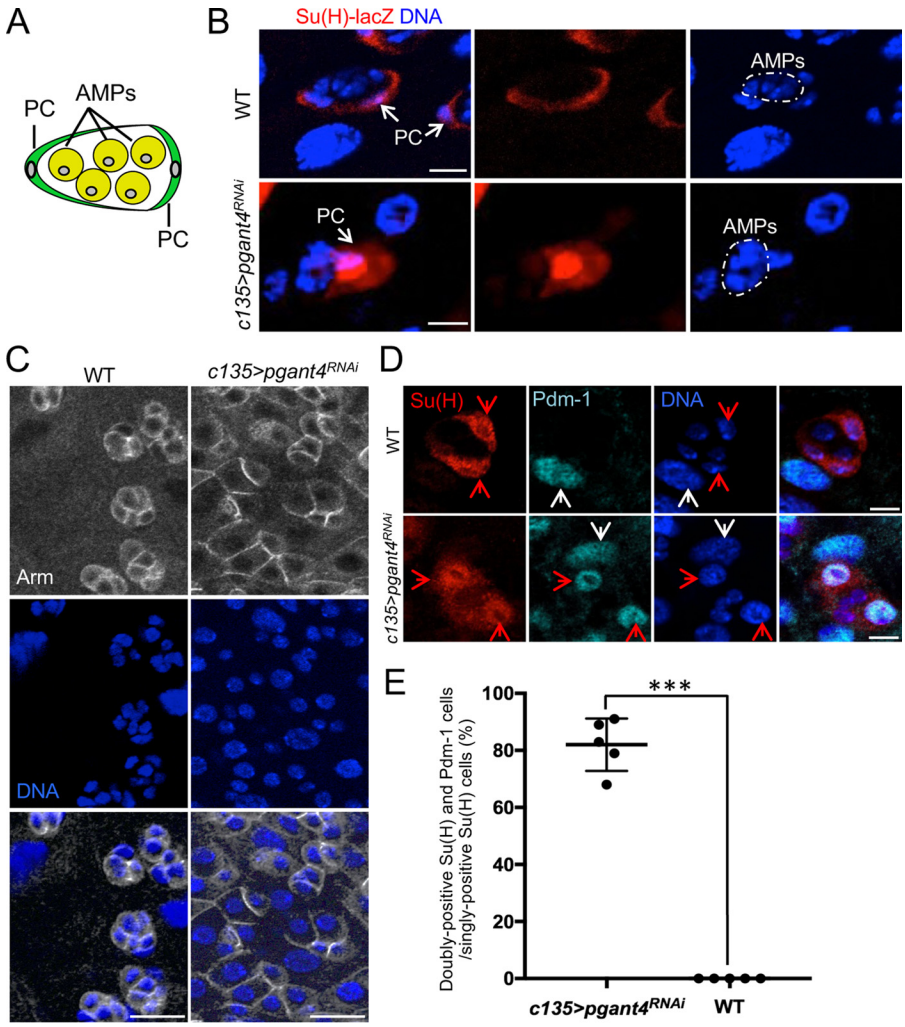


**Figure 2. Loss of the peritrophic membrane alters the progenitor cell niche.** *A*, diagram of PCs (*green*) wrapping AMPs (*yellow*) to form the progenitor cell niche. *B*, crescent-shaped PCs (as detected by the marker Su(H)-lacZ in *red*) are shown wrapping AMPs (*small blue nuclei*) in the WT (*Su(H)GBE-lacZ;c135*) third instar midgut. Upon loss of the peritrophic membrane (*Su(H)GBE-lacZ;c135>pgant4$^{RNAi}$*), PC shape is altered. AMP clusters (small nuclei without Su(H)-lacZ staining) are *outlined* with *dotted white lines*. *Scale bars*, 10 $\mu$m. *C*, Armadillo staining (Arm; *white*) outlines tight, distinct clusters of AMPs in the WT (*c135>VDRC60000*) midgut. Loss of the peritrophic membrane (*c135>pgant4$^{RNAi}$*) results in the loss of the small, tight clustering of AMPs that are no longer wrapped by PCs. Nuclear staining is shown in *blue*. *Scale bars*, 20 $\mu$m. *D*, PC fate is altered in the absence of the peritrophic membrane. Su(H)-positive PCs (*red*) do not express the EC marker, Pdm-1 (*cyan*), in the WT (*Su(H)GBE-lacZ;c135*) midgut. In the absence of the peritrophic membrane (*Su(H)GBE-lacZ; c135>pgant4$^{RNAi}$*), many Su(H)-positive PCs now also express Pdm-1. PCs are denoted by *red arrows*, and ECs are denoted by *white arrows*. Nuclear staining is shown in *blue*. *Scale bars*, 10 $\mu$m. *E*, quantitation of the percentage of doubly positive Su(H) and Pdm-1/singly positive Su(H) cells in a WT (*Su(H)GBE-lacZ;c135*) midgut and a midgut without the peritrophic membrane (*Su(H)GBE-lacZ;c135>pgant4$^{RNAi}$*). For each genotype, doubly positive Su(H) and Pdm-1 cells and singly positive Su(H) cells were counted in five third instar larval posterior midgut regions close to the junction between the midgut and hindgut as described under "Experimental procedures." Data are presented as the percentage of doubly positive Su(H) and Pdm-1 cells over singly positive Su(H) cells. Each *dot* represents the data from one larva. *Error bars*, S.D. ***, $p < 0.001$.

takes place within PCs and in some groups of AMPs in the absence of the peritrophic membrane. Taken together, our results suggest a model where loss of the protective mucinous peritrophic membrane results in epithelial cell damage and up-regulation of *upd3* expression specifically in EC cells, which in turn up-regulates JAK/STAT signaling in PCs, thereby altering the progenitor cell niche cell and causing an increase in progenitor cell proliferation.

To test this model, we first overexpressed *upd3* in ECs of WT larvae to determine if we could recapitulate the alteration of the progenitor cell niche and proliferation of the AMPs. As shown in Fig. 4, overexpression of *upd3* specifically in ECs (*Myo1A>UAS-upd3*) resulted in increased JAK/STAT signaling, aberrant PC morphology, and increased proliferation of AMPs relative to control (*Myo1A*) (Fig. 4, *A*, *B*, and *D*). By also using a UAS-GFP reporter (*Myo1A>UAS-upd3, UAS-GFP*), we found evidence for PC differentiation (as detected by the induction of expression of GFP in PCs that are still partially wrapping AMPs) when *upd3* was overexpressed (Fig. 4*C*). Expression of GFP under the control of the EC-specific promoter *Myo1A* is seen in PCs (*white arrows*) in *Myo1A>UAS-upd3, UAS-GFP* larvae but not in the absence of *upd3* overexpression (*Myo1A>UAS-GFP*). We next tested whether we could rescue the niche morphology and AMP proliferation seen upon loss of the peritrophic membrane by deleting *upd3*. In *pgant4* RNAi flies that carry a deletion for *upd3* (*Δupd3; c135>pgant4$^{RNAi}$*), JAK/STAT signaling was reduced (Fig. 5, *A* and *C*). Additionally, niche morphology was rescued (Fig. 5, *B*

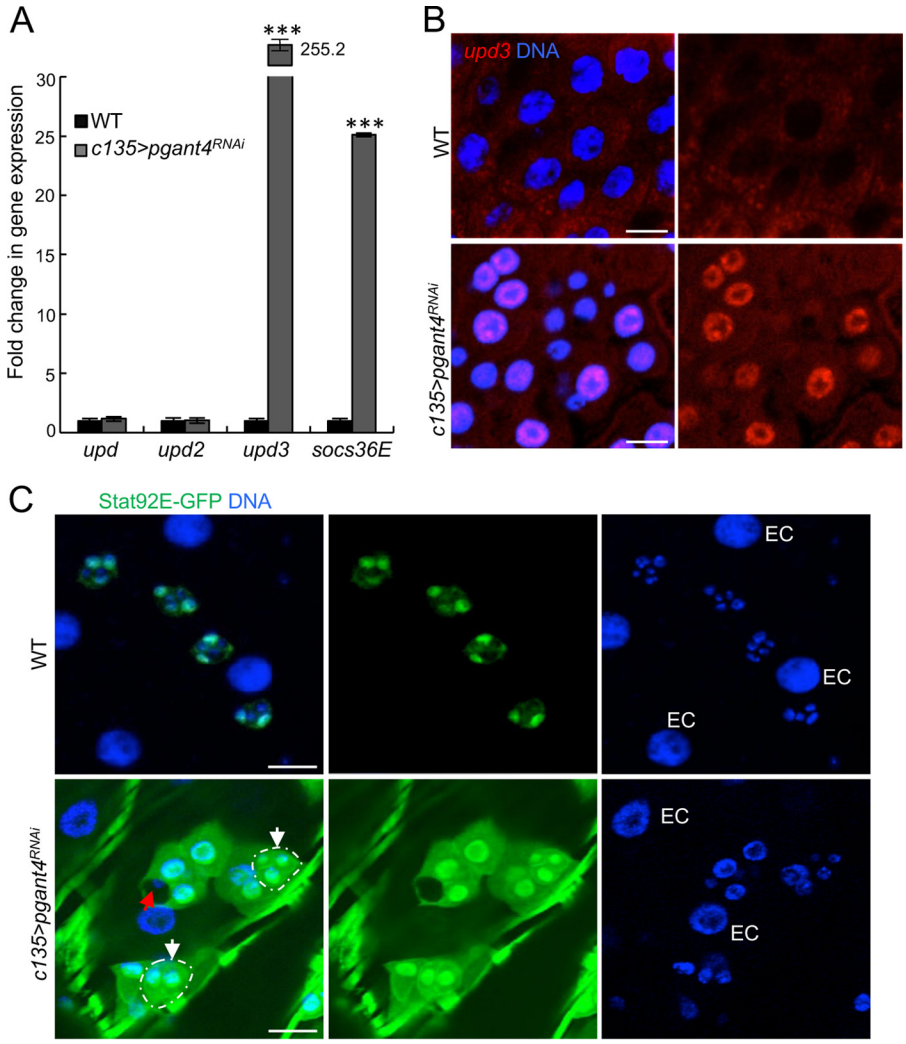


**Figure 3. Loss of the peritrophic membrane activates JAK/STAT signaling in niche cells and progenitor cells.** *A*, qPCR analysis shows a dramatic increase in expression of *upd3* and its downstream target *socs36E* in flies without peritrophic membrane (*c135>pgant4*$^{RNAi}$) relative to WT (*c135>VDRC60000*). *Error bars*, S.D. ***, $p < 0.001$. *B*, RNA *in situ* hybridization to *upd3* (*red*) reveals that it is expressed in ECs (large nuclei) in animals without peritrophic membrane (*c135>pgant4*$^{RNAi}$). No detectable expression of *upd3* was seen in WT. Nuclear staining is shown in *blue*. *Scale bars*, 20 $\mu$m. *C*, JAK/STAT signaling (as detected by the reporter Stat92E-GFP; *green*) is seen in the PCs (but not the AMPs) of the progenitor cell niche in the WT (*Stat92E-GFP, c135>VDRC60000*) third instar midgut. Upon loss of the peritrophic membrane (*Stat92E-GFP, c135>pgant4*$^{RNAi}$), JAK/STAT signaling is greatly increased in PCs, which now have a rounded morphology. Additionally, JAK/STAT signaling is now seen in some clusters of AMPs (*white circles* and *arrows*). The *red arrow* shows an AMP cluster that is still wrapped by a PC and is not JAK/STAT-positive. Cells with large nuclei (DNA, *blue*) are ECs. *Scale bars*, 20 $\mu$m.

and *C*), and AMP proliferation was significantly decreased (Fig. 5*D*).

To test whether the effects on JAK/STAT signaling and niche integrity were dependent upon the secreted peritrophic membrane, we next attempted to genetically restore the peritrophic membrane. Previous work from our group demonstrated that the defects in secretory vesicle formation and secretion of peritrophic membrane components in *pgant4* mutants were due to Dfur2-mediated proteolysis of the cargo receptor Tango1 and that secretory vesicle formation could be rescued by overexpression of Tango1 in PR cells of *pgant4* mutants (30). As shown in Fig. 6 (*A*–*C*), overexpression of *tango1* in PR cells in the *pgant4* RNAi background (*c135>pgant4*$^{RNAi}$, *tango1*$^{OE}$), restored the protective mucinous lining and rescued epithelial irregularities and apoptosis. Moreover, genetic restoration of the peritrophic membrane restored JAK/STAT signaling to wild-type levels and rescued aberrant proliferation (Fig. 6, *B* and *C*).

To determine whether this *in vivo* system could be used to test exogenous compounds that may function as mucin mimetics and restore epithelial cell integrity, we next fed purified mammalian mucins to *pgant4* mutant larvae. Larvae were fed either water ($H_2O$) or carboxymethylcellulose (CMC; a soluble derivative of cellulose that has viscous properties but lacks mucin-type glycans) as controls or mucins purified from pig intestine (Muc2) or stomach (Muc5AC). Muc2 is known to be crucial for digestive system function in mice (10). Interestingly, only Muc2 was able to reduce *upd3* expression and expression of its downstream target, *socs36E* (Fig. 6*D* and Fig. S5), suggesting that this particular mucin conferred protective properties to the digestive system. No reduction in *upd3* or JAK/STAT signaling was seen when using water or carboxymethylcellulose alone. Unexpectedly, Muc5AC actually increased *upd3* expression and JAK/STAT signaling, indicating that different mucins have distinct properties in terms of interaction with and/or protection of epithelial surfaces of the digestive tract.

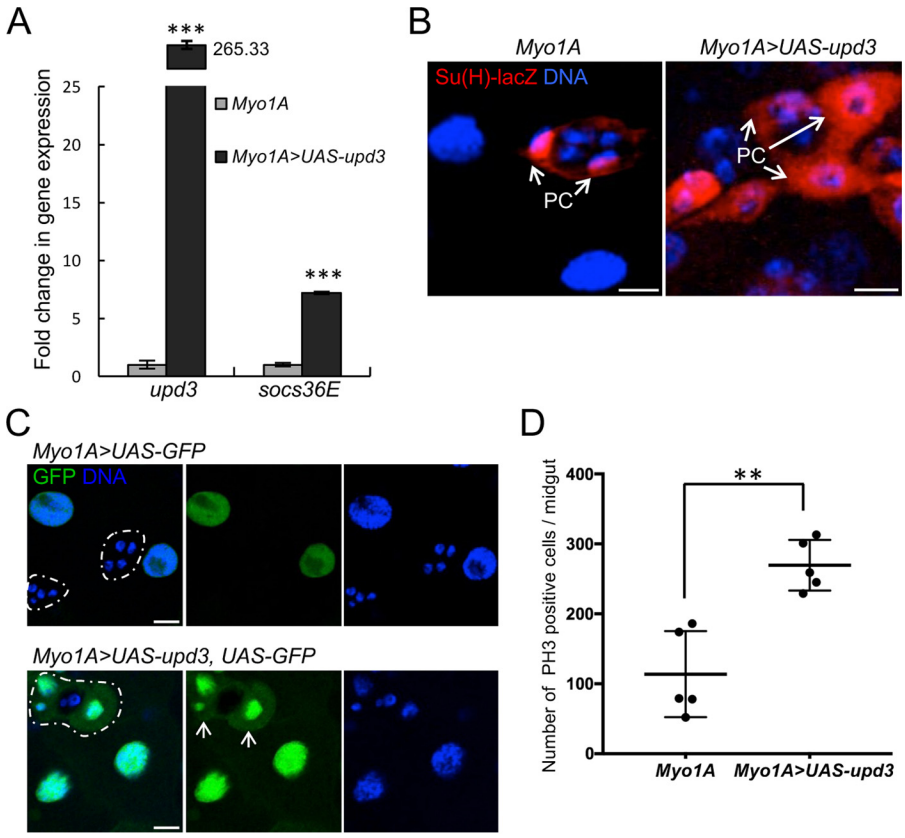


**Figure 4. Upd3 and JAK/STAT signaling are responsible for altered PC morphology and progenitor cell proliferation.** *A*, overexpression of *upd3* in ECs of WT larvae (*Myo1A>UAS-upd3*) resulted in the activation of JAK/STAT signaling as detected by increased expression of the downstream target *socs36E*. qPCR was performed by comparing gene expression between midguts of larvae overexpressing *upd3* (*Myo1A>UAS-upd3*) with those without *upd3* overexpression (*Myo1A*). *Error bars*, S.D. ***, $p < 0.001$. EC-based expression of *upd3* also resulted in altered PC morphology (as detected by the PC marker Su(H)-lacZ; *red*) (*B*) and PC differentiation (as detected by the induction of expression of GFP in PCs that are still partially wrapping AMPs in *Myo1A>UAS-upd3, UAS-GFP* larvae) (*C*). Clusters of PCs and AMPs are *outlined* with a *dotted white line* for each genotype. Expression of GFP under the control of the EC-specific promoter *Myo1A* is seen in PCs (*white arrows*) in *Myo1A>UAS-upd3, UAS-GFP* larvae but not in the absence of *upd3* overexpression (*Myo1A>UAS-GFP*). *D*, *upd3* overexpression (*Myo1A>UAS-upd3*) also increased cell proliferation relative to the control (*Myo1A*). *Error bars*, S.D. **, $p < 0.01$. *Scale bars*, 10 $\mu$m.

Finally, we tested the role of microbes in the increased JAK/STAT signaling and cell proliferation seen upon loss of the peritrophic membrane by treating *pgant4* RNAi larvae with antibiotics. Newly hatched WT or *c135>pgant4*$^{RNAi}$ first instar larvae were cultivated on food containing antibiotics and grown to third instar. As shown in Fig. 6*E*, treatment of *pgant4* RNAi larvae with antibiotics reduced the expression of antimicrobial genes to that of WT. Additionally, antibiotic treatment partially reduced *upd3* and *socs36E* expression as well as cell proliferation, suggesting that there is a microbial contribution to the cellular damage/changes seen upon loss of the peritrophic membrane (Fig. 6, *F* and *G*).

Taken together, our results demonstrate a crucial protective role for the mucinous peritrophic membrane of the *Drosophila* digestive tract. In the absence of this protective barrier, induction of *upd3* expression from epithelial cells increases JAK/STAT signaling within the progenitor cell niche that causes differentiation of PCs to EC-like cells, which alters the niche morphology and releases AMPs from their protective environment. AMPs are subsequently exposed to JAK/STAT signaling, which causes them to undergo aberrant cell proliferation (Fig. 7). Genetic restoration of this membrane rescues epithelial damage, JAK/STAT signaling, and niche integrity. Moreover, our studies suggest that this *in vivo* system could be used to screen for compounds and strategies that restore the functions of this protective barrier and/or modulate conserved signaling pathways.

## Discussion

Here, we demonstrate the crucial importance of the protective mucinous membrane in the integrity of the digestive epithelium and the maintenance of the progenitor cell niche. Whereas previous studies have investigated roles for components of this membrane in *Drosophila* (24), here we are able to completely eliminate it and monitor the ensuing cellular changes and signaling responses. We show the peritrophic membrane is essential to protect the integrity of the epithelial cell layer and maintain an appropriate environment for the progenitor cell niche. Moreover, we show a dynamic and specific response to the loss of this membrane via the production of the IL-6–like cytokine Upd3 from epithelial cells, which in turn signals to niche cells in a paracrine fashion, causing differentiation and morphological changes. This demonstrates the multipotent nature of PCs, which can respond to specific cytokines to alter their fate. Once the PC morphology and fate were altered, JAK/STAT signaling was activated in AMPs exposed to Upd3, causing aberrant cell proliferation/DNA replication (Fig. 7). This represents the first example where loss of the protective

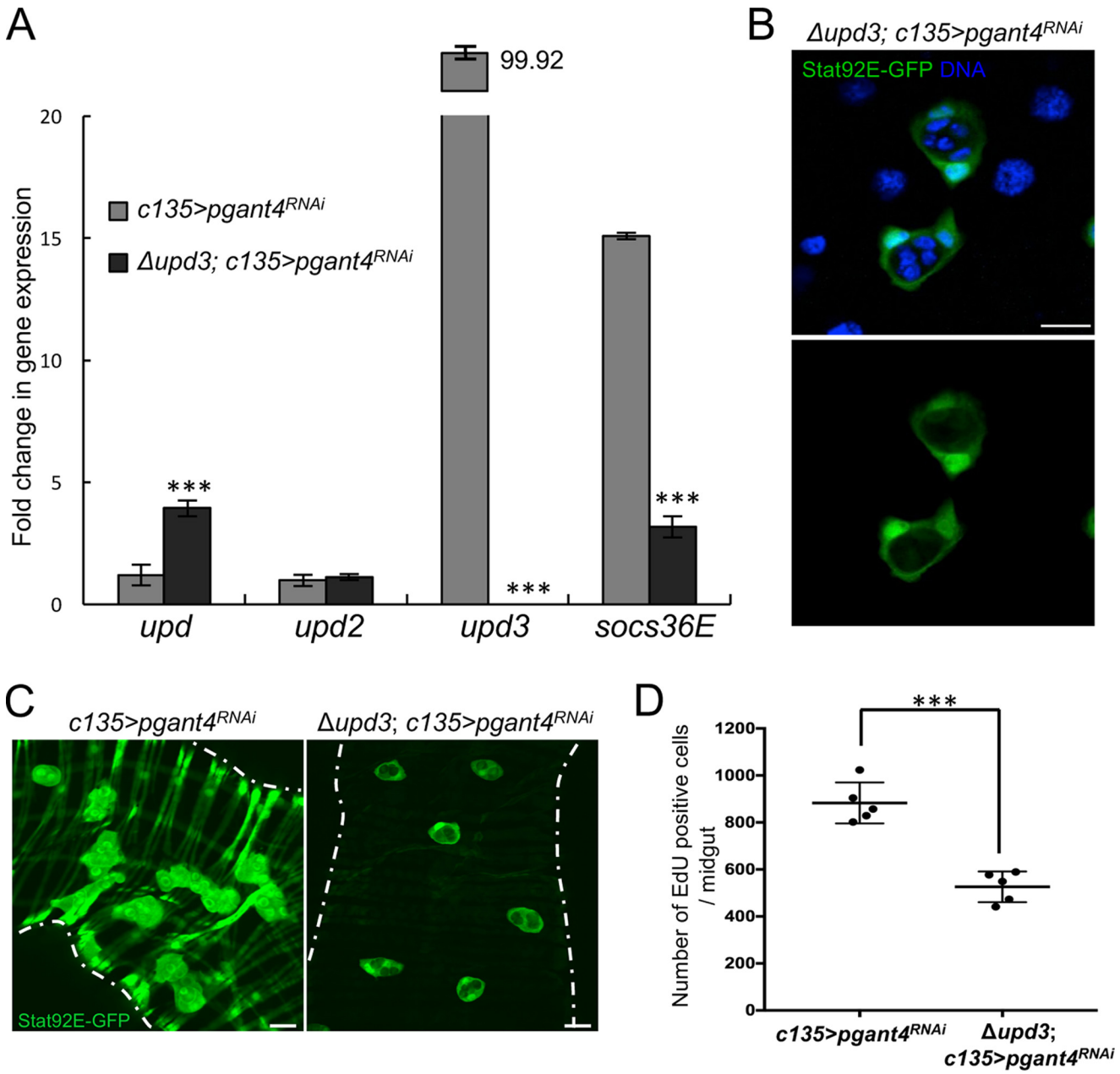


**Figure 5. Deletion of *upd3* in *pgant4* RNAi larvae reduces *socs36E* expression and rescues the progenitor cell niche.** *A*, qPCR analysis of gene expression in *c135>pgant4*$^{RNAi}$ and Δ*upd3; c135>pgant4*$^{RNAi}$ third instar midguts. Values were normalized to *rp49* and are plotted as -fold change in gene expression. *Error bars*, S.D. ***, $p < 0.001$. Niche cell morphology (*B*) and levels of JAK/STAT signaling (*C*) are restored in the *pgant4* RNAi background upon deletion of *upd3*, as detected by the Stat92E-GFP reporter (*green*) (compare *Stat92E-GFP, c135>pgant4*$^{RNAi}$ midguts with Δ*upd3; Stat92E-GFP, c135>pgant4*$^{RNAi}$ midguts). Nuclear staining (DNA) is shown in *blue*. *Scale bars*, 20 μM. *D*, deletion of *upd3* in larvae without peritrophic membrane (Δ*upd3; c135>pgant4*$^{RNAi}$) reduced cell proliferation within the midgut. EdU-positive cells were counted in five third instar larval midguts. Each *dot* represents one larva. *Error bars*, S.D. *Bar*, mean. ***, $p < 0.001$.

mucous lining activates signaling from epithelial cells to alter the fate of niche cells and change the behavior of progenitor cells. These studies highlight the importance of this membrane in both epithelial and progenitor cell biology and elucidate the paracrine signaling cascade that is specifically activated when this barrier is compromised.

Interestingly, the mucinous peritrophic membrane could be restored by overexpression of the conserved cargo receptor Tango1. Tango1 is an essential protein that functions to package large extracellular matrix proteins, such as collagen and mucins, into secretory vesicles (30, 31). Loss of the mammalian ortholog of Tango1 (Mia3) in a murine model resulted in lethality with global defects in collagen secretion and extracellular matrix composition (31). Alterations in Tango1/Mia3 expression have also been associated with colon and hepatocellular carcinomas in humans (32). Previous work in *Drosophila* demonstrated that PGANT4 glycosylates Tango1, protecting it from Dfur2-mediated proteolysis in the digestive tract (30). Here, we show that Tango1 overexpression specifically in the secretory PR cells of the digestive tract can restore the mucinous membrane throughout the midgut to rescue epithelial viability and niche integrity, further demonstrating the crucial role

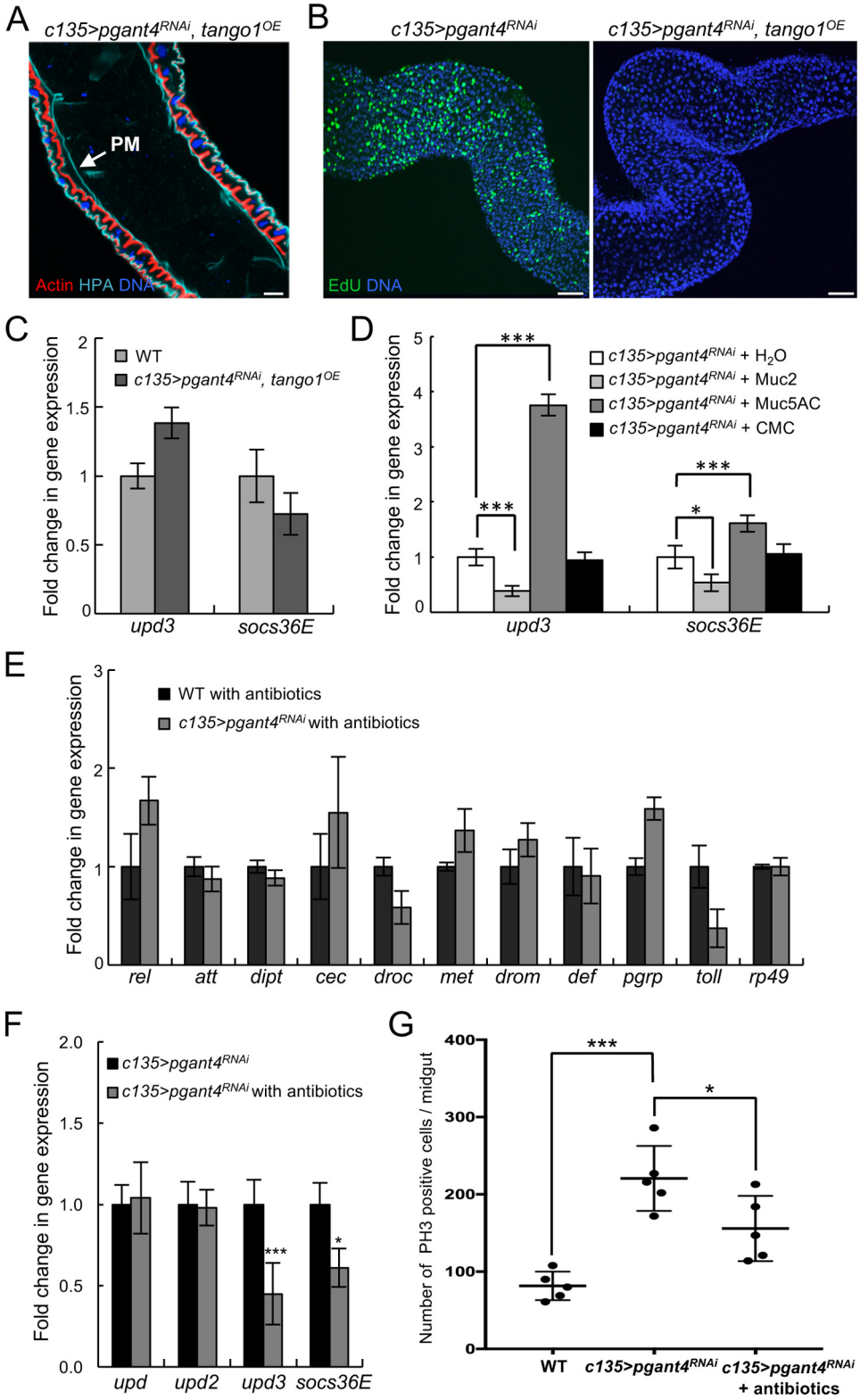


**Figure 6. Restoration of the peritrophic membrane rescues cell proliferation and JAK/STAT signaling.** Overexpression of the cargo receptor, Tango1, in PR cells of *c135>pgant4$^{RNAi}$* third instar larvae (*c135>pgant4$^{RNAi}$, tango1$^{OE}$*) restores the peritrophic membrane (as detected by the lectin *H. pomatia*; *cyan*) (*A*), rescues AMP proliferation (as detected by EdU; *green*) (*B*), and decreases *upd3* and *socs36E* expression levels to those of WT (*c135>VDRC60000*) (*C*). Actin (*red*) *outlines* the epithelial cell layer. *Scale bars*, 50 $\mu$m (*A*) and 20 $\mu$m (*B*). *D*, larvae deficient for *pgant4* were fed either water ($H_2O$), CMC, Muc2, or Muc5AC. Muc2 was the only compound that reduced *upd3* and *socs36E* expression in the *c135>pgant4$^{RNAi}$* background. Two additional independent trials are shown in Fig. S5. *E*, qPCR analysis of antimicrobial gene expression in WT (*c135>VDRC60000*) and peritrophic membrane-deficient larvae (*c135>pgant4$^{RNAi}$*) that were fed antibiotic-containing food. *F*, qPCR analysis reveals a decrease in *upd3* and *socs36E* gene expression when *c135>pgant4$^{RNAi}$* larvae are raised on antibiotic-containing food. Values were normalized to *rp49* and are plotted as -fold change in gene expression. *Error bars*, S.D. *G*, quantitation of proliferation (PH3-positive cells) within the midguts of WT larvae, *c135>pgant4$^{RNAi}$* larvae, and *c135>pgant4$^{RNAi}$* larvae raised on antibiotic-containing food. PH3-positive cells were counted in five third instar larval midguts. Each *dot* represents one larva. *Error bars*, S.D. *Bar*, mean. ***, $p < 0.001$; *, $p < 0.05$.

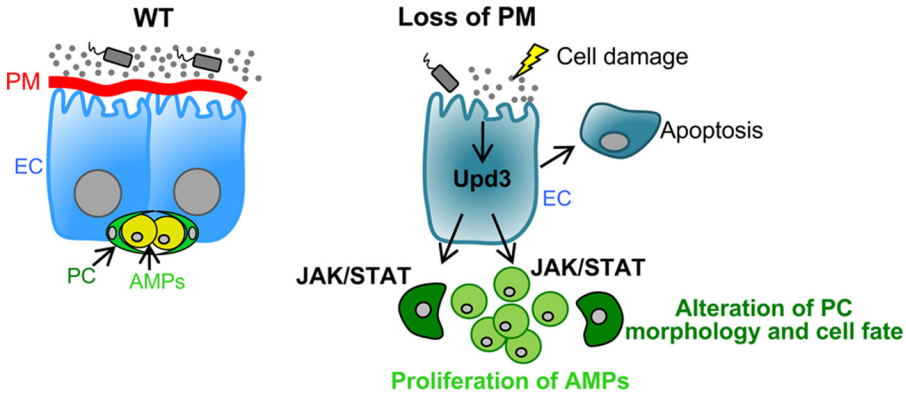


**Figure 7. Model depicting how loss of the peritrophic membrane (*PM*) affects epithelial cell integrity and the progenitor cell niche.** In the absence of the peritrophic membrane (*red*), ECs are exposed to mechanical and microbial insults, resulting in damage and the up-regulation of the IL-6-like cytokine, Upd3. Upd3 from ECs increases JAK/STAT signaling in PCs, resulting in changes in PC morphology and fate and disruption of the progenitor cell niche. Once the niche is disrupted, AMPs are exposed to Upd3, resulting in activation of JAK/STAT signaling and abnormal cell proliferation.

of the peritrophic membrane in digestive system homeostasis and health. These results suggest the possibility of exogenous Tango1 expression as a potential strategy to restore secretion, mucous membranes, and/or extracellular matrix composition and confer epithelial protection.

The larval digestive system offers unique opportunities to investigate the role of the individual components of the mucinous membrane and restorative strategies in epithelial biology. Unlike the adult stage, the larval portion of the life cycle is devoted to continuous feeding and digestion to orchestrate the massive growth of cells and tissues in preparation for metamorphosis (23). As such, larvae consume many types of solid food and will readily ingest various compounds. Indeed, oral supplementation with an intestinal mucin (Muc2) partially rescued JAK/STAT signaling, suggesting that this could serve as a strategy for epithelial protection. Muc2 is a major component of the protective mucous membrane that lines the small intestine and colon of mammals (2, 3). Muc2 is thought to confer lubrication for food passage as well as to form a barrier between microbes and epithelial cells of the digestive tract (2, 3). Our results suggest that Muc2 supplementation could be providing similar properties in the *Drosophila* digestive tract. Interestingly, supplementation with the gastric mucin (Muc5AC) dramatically exacerbated JAK/STAT signaling, suggesting that the different structural, rheological, or binding properties of each mucin are mediating distinct cellular responses in this system. Current work is focused on deciphering the specific functional regions of various secreted mucins and testing their ability to confer epithelial protection using this *in vivo* system.

Human diseases of the digestive tract are associated with disrupted mucinous linings, and disease severity is often correlated with the severity of barrier disruption (3, 16, 17). Interestingly, these diseases are also characterized by increased levels of the mammalian ortholog of Upd3 (IL-6), increased JAK/STAT activation, and increased cell proliferation (33–35), similar to what we see in *Drosophila*, suggesting conserved mechanisms for responding to mucosal disruption/injury. It is widely known that immune cells are one source of IL-6 in mammals, but recent studies have demonstrated that mechanically damaged epithelial and endothelial cells also produce IL-6 (36, 37). Here, we demonstrate that epithelial expression of Upd3 is both necessary and sufficient for the changes in PC fate and AMP proliferation, as disruption of the niche could be recapitulated by overexpression of *upd3* from ECs and rescued by deletion of *upd3*. How peritrophic membrane loss is signaling to up-regulate *upd3* expression in ECs is currently unknown. However, previous studies in the adult *Drosophila* digestive system have shown up-regulation of *upd*, *upd2*, and *upd3* in response to enteric infection or damage-inducing agents, such as bleomycin or dextran sulfate sodium (38–41), suggesting roles for both microbial insults and physical/mechanical damage to epithelial cells. Indeed, our results also suggest roles for microbial and mechanical damage in the absence of the peritrophic membrane, as both antibiotics and mucin supplementation were able to reduce *upd3* expression and cell proliferation. This study demonstrates that the larval midgut can serve as a model system to study how cells/tissues sense and respond to damage as well as to decipher how *upd3* is specifically activated in epithelial cells under various conditions.

As a mucous layer is present across most internal epithelial surfaces of our bodies, understanding the mechanisms by which it confers protection and epithelial homeostasis will inform us in treating various diseases affecting the integrity of this layer. Mucosal healing has been proposed as a treatment option for inflammatory bowel disease and other diseases of the digestive tract that are characterized by destruction of the mucosa and epithelial surfaces (42). Likewise, mucins are a component in some oral treatments for dry mouth caused by head and neck irradiation or Sjogren's syndrome (43). Other therapeutics for various autoimmune and inflammatory diseases include JAK inhibitors (Jakinibs) and drugs directed against particular cytokines (44, 45). In this study, we show that genetic restoration of the peritrophic membrane can restore digestive system health and that antibiotic treatment or mucin supplementation can partially rescue damage-induced signaling cascades, suggesting that this *Drosophila* system may be a viable platform for testing compounds to remediate epithelial damage. Future studies will focus on testing newly emerging mucin mimetics (designed to confer epithelial protection and appropriate rheology/hydration), synthetic mucins (where the extent of glycosylation can be specifically modified) (46), glycan-based hydrogels (47), and drugs that target conserved steps

in the JAK/STAT signaling cascade (44). Lessons learned in *Drosophila* may inform future strategies for functional restoration of mucosal protection.

### Experimental procedures

#### Fly strains

The stocks used in this study are listed below. The Bloomington stocks used were 6978 ($w^{1118}$;*P{GawB}c135* or *c135*, the proventriculus-Gal4 driver line); 5 (Oregon-R-C), 18521 ($pgant4^{f02186}$, the transposon insertion in *pgant4*); 6502 (*Df(2L) tim-02/CyO*, the gene deficiency line of *pgant4*); 55728 ($w^{*}$; Δ*upd3*); and 10359 ($y^{1}$ $w^{67c23}$;*P{lacW}esg*$^{k00606}$/*CyO*). The Vienna *Drosophila* RNAi Center (VDRC) stocks used were 7286 ($pgant4^{RNAi}$ line) and 60000 ($w^{1118}$, the wild-type control for RNAi experiments). The *10xStat92E-GFP* (*Stat92E-GFP*) stock (48); *FM7Tub-Gal80*$^{ts}$, *Myo1A-Gal4, UAS-GFP/CyO* stock (49); and *Su(H)GBE-lacZ* stock (50) were kind gifts of Dr. N. Perrimon. The *Myo1A-Gal4, Tub-Gal80*$^{ts}$ stock (51) was the kind gift of Dr. S. Hou. The *w; UAS-upd3/CyO* stock (41) was the kind gift of Dr. N. Buchon. The *tango1*$^{OE}$ stock was described previously (30).

#### Quantitative real-time PCR

Primers used are from the DRSC FlyPrimerBank (http://www.flyrnai.org/flyprimerbank)[4] (56). To examine gene expression levels, midguts of third instar larvae were used to isolate RNA and perform real-time PCR. Briefly, RNA was isolated from 15 midguts of the proper genotype or condition using the RNAqueous-Micro kit (Invitrogen). cDNA synthesis was performed using the iScript cDNA synthesis kit (Bio-Rad). Quantitative RT-PCR was performed on a MyiQ real-time PCR thermocycler (Bio-Rad) using the SYBR Green PCR Master Mix (Bio-Rad). Analyzed products were assayed in triplicate and in multiple independent experiments. Data are presented as mean values, and *error bars* represent S.D.

#### In situ hybridization

*upd3* RNA probes were prepared as described previously (52) and labeled using the DIG labeling kit (Roche Applied Science). *Drosophila* third instar larval midguts were dissected and fixed in 4% PFA/PBS with 0.6% Triton X-100. After fixation and washing, whole-mount midgut *in situ* hybridization was performed. Briefly, fixed guts were rinsed in hybridization buffer/PBST (PBS with 0.1% Tween 20) and then incubated with hybridization buffer at 60 °C for 1 h. Hybridization was performed by incubating with denatured 100 ng/ml DIG RNA probes at 60 °C overnight. Guts were washed the next day and incubated with anti-DIG-POD (horseradish peroxidase) antibody (Roche Applied Science; 1:100) at 4 °C overnight. Guts were washed and incubated with tyramide signal amplification plus Cy3 (PerkinElmer Life Sciences; 1:50 by amplification buffer) for 1 h. Finally, samples were washed with PBST and mounted with Vectashield mounting medium with DAPI (Vector Laboratories) and stored at 4 °C.

[4] Please note that the JBC is not responsible for the long-term archiving and maintenance of this site or any other third party hosted site.

#### Whole-mount staining of midguts

Guts were dissected from third instar larvae and fixed in 4% formaldehyde in PBS. Samples were washed in PBST (PBS plus 0.3% Triton X-100) and transferred to blocking buffer (2% BSA, PBS, 0.3% Triton X-100) for 1 h on a shaker. Primary antibodies used were anti-GFP (Abcam; 1:2000), anti-Arm (DSHB; 1:10), anti-Dl (DSHB C594.9B; 1:150), anti-Pdm1 (53) (kind gift of Dr. Y. Cai; 1:250), anti-phospho-histone H3 (Cell Signaling Technology; 1:1000), anti-β-Gal (Abcam; 1:1000), and anti-Dcp1 (Cell Signaling Technology; 1:100). Samples were incubated with primary antibody overnight at 4 °C in blocking buffer and incubated with anti-rabbit or mouse IgG antibody (Jackson ImmunoResearch Laboratories; 1:100), or anti-chicken IgY antibody (Abcam; 1:2000) at room temperature for 4 h. Counterstaining was performed using HPA-488 (Thermo Fisher Scientific; 1:1000) and TRITC-phalloidin (Sigma; 1:100). For the Dl antibody staining, primary antibody incubation was followed by fluorescent detection using the tyramide signal amplification kit (ThermoFisher Scientific) according to the manufacturer's instructions. Samples were mounted in aqueous mounting medium with Vectashield mounting medium with DAPI (Vector Laboratories) on a slide with a spacer and imaged on a Zeiss LSM 510 confocal microscope or Nikon A1R confocal microscope. Images were processed using the LSM Imager Browser and ImageJ.

#### EdU staining analysis

Briefly, midguts were dissected from third instar larvae and incubated in medium (Schneider's + 10% FBS) with 10 μM EdU (Invitrogen) for 45 min at room temperature. The following steps were performed according to the manufacturer's instructions. After incubation, tissues were fixed in 4% paraformaldehyde, washed in 3% BSA, and permeabilized in 0.5% Triton X-100. Then guts were incubated in Click-iT reaction mixture. After washing, samples were mounted in aqueous mounting medium with Vectashield mounting medium with DAPI (Vector Laboratories) on a slide with a spacer and imaged on a Zeiss LSM 510 confocal microscope or Nikon A1R confocal microscope. Images were processed using the LSM Imager Browser and ImageJ.

#### Cell counting

Cell proliferation was quantified by counting PH3 antibody or EdU-stained cells in five third instar larval midguts of each genotype under the appropriate conditions. Individual data points and mean values were shown. For the niche cell differentiation analysis, doubly positive Su(H) and Pdm-1 cells and singly positive Su(H) cells were counted in five third instar larval posterior midguts of each genotype. We analyzed the region of the posterior midgut ~40 μm from the junction of the midgut and hindgut. Cells were scored in three areas (each of 100 × 100 μm) within the posterior midgut of each larvae of each genotype to generate the data shown in Fig. 2*E*. Data are presented as the percentage of doubly positive Su(H) and Pdm-1 cells over singly positive Su(H) cells.

### *Mucin purification and feeding*

Porcine intestinal and gastric mucins were isolated by the previously described protocol (54, 55) but excluding the cesium chloride density gradient ultracentrifugation. Briefly, mucus was removed from the epithelial surface of pig tissues by gentle scraping and then solubilized in the presence of saline and protease inhibitors. Insoluble debris was removed by centrifugation, and the high-molecular weight, periodic acid–Schiff–positive glycoproteins were isolated in the void volume fractions from Sepharose CL2B size-exclusion chromatography, followed by ultrafiltration and lyophilization. Muc2 and Muc5AC glycoproteins were verified by mass spectrometry as the predominant mucin species in the isolated intestinal and gastric mucins preparations, respectively. Fly crosses were performed on egg lay plates as described (52). Eggs were then transferred to tubes containing food mixed with either purified mucins (600 $\mu$l of 5 mg/ml mucin added to 1 g of MM media from KD Medical), carboxymethylcellulose (600 $\mu$l of 5 mg/ml CMC added to 1 g of MM media), or water (600 $\mu$l added to 1 g of MM media). After 3 days of feeding, midguts were dissected from 15 larvae, and RNA was extracted for real-time PCR.

### *Antibiotic feeding*

Crossed flies were set up in vials containing food (MM media, KD Medical) with antibiotics (penicillin (100 units/ml) and streptomycin (0.1 mg/ml)). After egg laying, parents were removed, and progeny were incubated in the bottle for an additional ~3–4 days. 15 midguts from each treatment were dissected from third instar larvae, and cell proliferation and gene expression were examined. Four independent feeding experiments were performed.

### *Statistics*

Experiments were performed three or more times, and averages for each experiment were calculated. *Error bars* represent S.D., and significance values were calculated using Student's *t* test or analysis of variance for comparison of data from three or more groups. *, $p < 0.05$; **, $p < 0.01$; ***, $p < 0.001$.

*Author contributions*—L. Z. and K. G. T. H. designed all experiments. L. Z. carried out all experiments shown. K. R. and B. T. purified and characterized the mucins. K. G. T. H. wrote the manuscript, with assistance from L. Z. and K. R.

*Acknowledgments—We thank the members of our laboratory for comments and feedback. We also thank Drs. L. Tabak and D. Tran for many helpful discussions and insight. We thank Drs. N. Perrimon, S. Hou, and N. Buchon for the fly stocks and Dr. Y. Cai for the Pdm-1 antibody. We also thank the Vienna Drosophila RNAi Center, the Bloomington Stock Center, and the Developmental Studies Hybridoma Bank for fly stocks and other reagents.*

### References

1. Hansson, G. C. (2012) Role of mucus layers in gut infection and inflammation. *Curr. Opin. Microbiol.* **15,** 57–62
2. Johansson, M. E., and Hansson, G. C. (2016) Immunological aspects of intestinal mucus and mucins. *Nat. Rev. Immunol.* **16,** 639–649
3. Johansson, M. E., Sjövall, H., and Hansson, G. C. (2013) The gastrointestinal mucus system in health and disease. *Nat. Rev. Gastroenterol. Hepatol.* **10,** 352–361
4. McGuckin, M. A., Lindén, S. K., Sutton, P., and Florin, T. H. (2011) Mucin dynamics and enteric pathogens. *Nat. Rev. Microbiol.* **9,** 265–278
5. Arike, L., and Hansson, G. C. (2016) The densely *O*-glycosylated MUC2 mucin protects the intestine and provides food for the commensal bacteria. *J. Mol. Biol.* **428,** 3221–3229
6. Corfield, A. P. (2015) Mucins: a biologically relevant glycan barrier in mucosal protection. *Biochim. Biophys. Acta* **1850,** 236–252
7. Tabak, L. A. (1995) In defense of the oral cavity: structure, biosynthesis, and function of salivary mucins. *Annu. Rev. Physiol.* **57,** 547–564
8. Syed, Z. A., Härd, T., Uv, A., and van Dijk-Härd, I. F. (2008) A potential role for *Drosophila* mucins in development and physiology. *PLoS One* **3,** e3041
9. Roy, M. G., Livraghi-Butrico, A., Fletcher, A. A., McElwee, M. M., Evans, S. E., Boerner, R. M., Alexander, S. N., Bellinghausen, L. K., Song, A. S., Petrova, Y. M., Tuvim, M. J., Adachi, R., Romo, I., Bordt, A. S., Bowden, M. G., *et al.* (2014) Muc5b is required for airway defence. *Nature* **505,** 412–416
10. Velcich, A., Yang, W., Heyer, J., Fragale, A., Nicholas, C., Viani, S., Kucherlapati, R., Lipkin, M., Yang, K., and Augenlicht, L. (2002) Colorectal cancer in mice genetically deficient in the mucin Muc2. *Science* **295,** 1726–1729
11. Chaudhury, N. M., Proctor, G. B., Karlsson, N. G., Carpenter, G. H., and Flowers, S. A. (2016) Reduced mucin-7 (Muc7) sialylation and altered saliva rheology in Sjogren's syndrome associated oral dryness. *Mol. Cell. Proteomics* **15,** 1048–1059
12. Chaudhury, N. M., Shirlaw, P., Pramanik, R., Carpenter, G. H., and Proctor, G. B. (2015) Changes in saliva rheological properties and mucin glycosylation in dry mouth. *J. Dent. Res.* **94,** 1660–1667
13. Bergstrom, K., Liu, X., Zhao, Y., Gao, N., Wu, Q., Song, K., Cui, Y., Li, Y., McDaniel, J. M., McGee, S., Chen, W., Huycke, M. M., Houchen, C. W., Zenewicz, L. A., West, C. M., *et al.* (2016) Defective intestinal mucin-type *O*-glycosylation causes spontaneous colitis-associated cancer in mice. *Gastroenterology* **151,** 152–164.e11
14. Gao, N., Bergstrom, K., Fu, J. X., Xie, B., Chen, W. C., and Xia, L. J. (2016) Loss of intestinal *O*-glycans promotes spontaneous duodenal tumors. *Am. J. Physiol. Gastrointest. Liver Physiol.* **311,** G74–G83
15. Van der Sluis, M., De Koning, B. A. E., De Bruijn, A. C. J. M., Velcich, A., Meijerink, J. P. P., Van Goudoever, J. B., Büller, H. A., Dekker, J., Van Seuningen, I., Renes, I. B., and Einerhand, A. W. C. (2006) Muc2-deficient mice spontaneously develop colitis, indicating that Muc2 is critical for colonic protection. *Gastroenterology* **131,** 117–129
16. Guda, K., Moinova, H., He, J., Jamison, O., Ravi, L., Natale, L., Lutterbaugh, J., Lawrence, E., Lewis, S., Willson, J. K. V., Lowe, J. B., Wiesner, G. L., Parmigiani, G., Barnholtz-Sloan, J., Dawson, D. W., *et al.* (2009) Inactivating germ-line and somatic mutations in polypeptide *N*-acetylgalactosaminyltransferase 12 in human colon cancers. *Proc. Natl. Acad. Sci. U.S.A.* **106,** 12921–12925
17. Larsson, J. M. H., Karlsson, H., Crespo, J. G., Johansson, M. E. V., Eklund, L., Sjövall, H., and Hansson, G. C. (2011) Altered *O*-glycosylation profile of MUC2 mucin occurs in active ulcerative colitis and is associated with increased inflammation. *Inflamm. Bowel Dis.* **17,** 2299–2307
18. Bennett, E. P., Mandel, U., Clausen, H., Gerken, T. A., Fritz, T. A., and Tabak, L. A. (2012) Control of mucin-type *O*-glycosylation: a classification of the polypeptide GalNAc-transferase gene family. *Glycobiology* **22,** 736–756
19. Lang, T., Hansson, G. C., and Samuelsson, T. (2007) Gel-forming mucins appeared early in metazoan evolution. *Proc. Natl. Acad. Sci. U.S.A.* **104,** 16209–16214
20. Ten Hagen, K. G., Tran, D. T., Gerken, T. A., Stein, D. S., and Zhang, Z. (2003) Functional characterization and expression analysis of members of the UDP-GalNAc:polypeptide *N*-acetylgalactosaminyltransferase family from *Drosophila* melanogaster. *J. Biol. Chem.* **278,** 35039–35048
21. ten Hagen, K. G., Zhang, L., Tian, E., and Zhang, Y. (2009) Glycobiology on the fly: developmental and mechanistic insights from *Drosophila*. *Glycobiology* **19,** 102–111

22. Lehane, M. J. (1997) Peritrophic matrix structure and function. *Annu. Rev. Entomol.* **42,** 525–550
23. Lemaitre, B., and Miguel-Aliaga, I. (2013) The digestive tract of *Drosophila melanogaster*. *Annu. Rev. Genet* **47,** 377–404
24. Kuraishi, T., Binggeli, O., Opota, O., Buchon, N., and Lemaitre, B. (2011) Genetic evidence for a protective role of the peritrophic matrix against intestinal bacterial infection in *Drosophila melanogaster*. *Proc. Natl. Acad. Sci. U.S.A.* **108,** 15966–15971
25. Fox, D. T., and Spradling, A. C. (2009) The *Drosophila* hindgut lacks constitutively active adult stem cells but proliferates in response to tissue damage. *Cell Stem Cell* **5,** 290–297
26. Jiang, H., and Edgar, B. A. (2011) Intestinal stem cells in the adult *Drosophila* midgut. *Exp. Cell Res.* **317,** 2780–2788
27. Marianes, A., and Spradling, A. C. (2013) Physiological and stem cell compartmentalization within the *Drosophila* midgut. *Elife* **2,** e00886
28. Mathur, D., Bost, A., Driver, I., and Ohlstein, B. (2010) A transient niche regulates the specification of *Drosophila* intestinal stem cells. *Science* **327,** 210–213
29. Takashima, S., and Hartenstein, V. (2012) Genetic control of intestinal stem cell specification and development: a comparative view. *Stem Cell Rev.* **8,** 597–608
30. Zhang, L., Syed, Z. A., van Dijk Härd, I., Lim, J. M., Wells, L., and Ten Hagen, K. G. (2014) *O*-Glycosylation regulates polarized secretion by modulating Tango1 stability. *Proc. Natl. Acad. Sci. U.S.A.* **111,** 7296–7301
31. Wilson, D. G., Phamluong, K., Li, L., Sun, M., Cao, T. C., Liu, P. S., Modrusan, Z., Sandoval, W. N., Rangell, L., Carano, R. A., Peterson, A. S., and Solloway, M. J. (2011) Global defects in collagen secretion in a Mia3/TANGO1 knockout mouse. *J. Cell Biol.* **193,** 935–951
32. Arndt, S., and Bosserhoff, A. K. (2007) Reduced expression of TANGO in colon and hepatocellular carcinomas. *Oncol. Rep.* **18,** 885–891
33. Slattery, M. L., Lundgreen, A., Kadlubar, S. A., Bondurant, K. L., and Wolff, R. K. (2013) JAK/STAT/SOCS-signaling pathway and colon and rectal cancer. *Mol. Carcinog.* **52,** 155–166
34. Yu, H., Lee, H., Herrmann, A., Buettner, R., and Jove, R. (2014) Revisiting STAT3 signalling in cancer: new and unexpected biological functions. *Nat. Rev. Cancer* **14,** 736–746
35. Grivennikov, S., Karin, E., Terzic, J., Mucida, D., Yu, G. Y., Vallabhapurapu, S., Scheller, J., Rose-John, S., Cheroutre, H., Eckmann, L., and Karin, M. (2009) IL-6 and Stat3 are required for survival of intestinal epithelial cells and development of colitis-associated cancer. *Cancer Cell* **15,** 103–113
36. Dutzan, N., Abusleme, L., Bridgeman, H., Greenwell-Wild, T., Zangerle-Murray, T., Fife, M. E., Bouladoux, N., Linley, H., Brenchley, L., Wemyss, K., Calderon, G., Hong, B. Y., Break, T. J., Bowdish, D. M., Lionakis, M. S., *et al.* (2017) On-going Mechanical Damage from Mastication Drives Homeostatic Th17 Cell Responses at the Oral Barrier. *Immunity* **46,** 133–147
37. Kobayashi, S., Nagino, M., Komatsu, S., Naruse, K., Nimura, Y., Nakanishi, M., and Sokabe, M. (2003) Stretch-induced IL-6 secretion from endothelial cells requires NF-κB activation. *Biochem. Biophys. Res. Commun.* **308,** 306–312
38. Guo, Z., Driver, I., and Ohlstein, B. (2013) Injury-induced BMP signaling negatively regulates *Drosophila* midgut homeostasis. *J. Cell Biol.* **201,** 945–961
39. Jiang, H., Patel, P. H., Kohlmaier, A., Grenley, M. O., McEwen, D. G., and Edgar, B. A. (2009) Cytokine/Jak/Stat signaling mediates regeneration and homeostasis in the *Drosophila* midgut. *Cell* **137,** 1343–1355
40. Tian, A., Shi, Q., Jiang, A., Li, S., Wang, B., and Jiang, J. (2015) Injury-stimulated Hedgehog signaling promotes regenerative proliferation of *Drosophila* intestinal stem cells. *J. Cell Biol.* **208,** 807–819
41. Zhou, F., Rasmussen, A., Lee, S., and Agaisse, H. (2013) The UPD3 cytokine couples environmental challenge and intestinal stem cell division through modulation of JAK/STAT signaling in the stem cell microenvironment. *Dev. Biol.* **373,** 383–393
42. Neurath, M. F. (2014) New targets for mucosal healing and therapy in inflammatory bowel diseases. *Mucosal Immunol.* **7,** 6–19
43. Harvey, N. M., Yakubov, G. E., Stokes, J. R., and Klein, J. (2011) Normal and shear forces between surfaces bearing porcine gastric mucin, a high-molecular-weight glycoprotein. *Biomacromolecules* **12,** 1041–1050
44. Schwartz, D. M., Bonelli, M., Gadina, M., and O'Shea, J. J. (2016) Type I/II cytokines, JAKs, and new strategies for treating autoimmune diseases. *Nat. Rev. Rheumatol.* **12,** 25–36
45. Wang, S. W., and Sun, Y. M. (2014) The IL-6/JAK/STAT3 pathway: potential therapeutic strategies in treating colorectal cancer (Review). *Int. J. Oncol.* **44,** 1032–1040
46. Kramer, J. R., Onoa, B., Bustamante, C., and Bertozzi, C. R. (2015) Chemically tunable mucin chimeras assembled on living cells. *Proc. Natl. Acad. Sci. U.S.A.* **112,** 12574–12579
47. Lohmann, N., Schirmer, L., Atallah, P., Wandel, E., Ferrer, R. A., Werner, C., Simon, J. C., Franz, S., and Freudenberg, U. (2017) Glycosaminoglycan-based hydrogels capture inflammatory chemokines and rescue defective wound healing in mice. *Sci. Transl. Med.* **9,** eaai9044
48. Bach, E. A., Ekas, L. A., Ayala-Camargo, A., Flaherty, M. S., Lee, H., Perrimon, N., and Baeg, G. H. (2007) GFP reporters detect the activation of the *Drosophila* JAK/STAT pathway *in vivo*. *Gene Expr. Patterns* **7,** 323–331
49. Karpowicz, P., Perez, J., and Perrimon, N. (2010) The Hippo tumor suppressor pathway regulates intestinal stem cell regeneration. *Development* **137,** 4135–4145
50. Micchelli, C. A., and Perrimon, N. (2006) Evidence that stem cells reside in the adult *Drosophila* midgut epithelium. *Nature* **439,** 475–479
51. Zeng, X., Han, L., Singh, S. R., Liu, H., Neumüller, R. A., Yan, D., Hu, Y., Liu, Y., Liu, W., Lin, X., and Hou, S. X. (2015) Genome-wide RNAi screen identifies networks involved in intestinal stem cell regulation in *Drosophila*. *Cell Rep.* **10,** 1226–1238
52. Tian, E., and Ten Hagen, K. G. (2006) Expression of the UDP-GalNAc: polypeptide *N*-acetylgalactosaminyltransferase family is spatially and temporally regulated during *Drosophila* development. *Glycobiology* **16,** 83–95
53. Zhou, J., Florescu, S., Boettcher, A. L., Luo, L., Dutta, D., Kerr, G., Cai, Y., Edgar, B. A., and Boutros, M. (2015) Dpp/Gbb signaling is required for normal intestinal regeneration during infection. *Dev. Biol.* **399,** 189–203
54. Caldara, M., Friedlander, R. S., Kavanaugh, N. L., Aizenberg, J., Foster, K. R., and Ribbeck, K. (2012) Mucin biopolymers prevent bacterial aggregation by retaining cells in the free-swimming state. *Curr. Biol.* **22,** 2325–2330
55. Celli, J., Gregor, B., Turner, B., Afdhal, N. H., Bansil, R., and Erramilli, S. (2005) Viscoelastic properties and dynamics of porcine gastric mucin. *Biomacromolecules* **6,** 1329–1333
56. Hu, Y., Sopko, R., Foos, M., Kelley, C., Flockhart, I., Ammeux, N., Wang, X., Perkins, L., Perrimon, N., and Mohr, S. E. (2013) FlyPrimerBank: an online database for *Drosophila melanogaster* gene expression analysis and knockdown evaluation of RNAi reagents. *G3* (*Bethesda*) **3,** 1607–1616